Eur. Phys. J. D **9**, 643–646 (1999)

THE EUROPEAN PHYSICAL JOURNAL D

EDP Sciences

Longitudinal modes of quantum dots in magnetic fields

Ll. Serra[1], M. Pi[2], A. Emperador[2], M. Barranco[2], and E. Lipparini[3]

[1] Departament de Física, Universitat de les Illes Balears, E-07071 Palma de Mallorca, Spain
[2] Departament d'Estructura i Constituents de la Matèria, Facultat de Física, Universitat de Barcelona, E-08028 Barcelona, Spain
[3] Dipartimento di Fisica, Università di Trento and INFM Sezione di Trento, I-38050 Povo, Italy

Received: 31 August 1998 / Received in final form: 11 January 1999

Abstract. The far infrared longitudinal spin and density responses of two-dimensional quantum dots are discussed within local spin-density functional theory. The influence of a partial spin polarization, induced by a perpendicular static magnetic field, is taken into account in the coupling of spin and density channels. As an illustrative application, the case of a dot made of 5 electrons in parabolic confinement is discussed.

PACS. 73.20.Dx Electron states in low-dimensional structures – 78.20.Bh Theory, models and numerical simulation

1 Introduction

Collective excitations induced in finite Fermi systems by external probes are a subject of widespread interest because, in general, they provide relevant information about the structure and interactions of these systems. For instance, particular effort has been devoted to the study of plasmon modes in the optical spectrum of metallic clusters [1]. Recent progress in the fabrication of semiconductor structures has allowed the extension of these studies to low-dimensional electronic systems. For two-dimensional (2D) quantum dots, the experiments carried out by Sikorski and Merkt [2] and by Demel *et al.* [3], as well as subsequent theoretical works [4–7], have shown that the far infrared excitation spectrum of these systems is dominated by dipole edge magnetoplasmon peaks. These are density (charge) modes excited by the dipole operator $D_\varrho = \sum_i x_i$, with the 2D dot located in the xy plane, that split into two different dispersion branches when a magnetic field B is applied perpendicularly to the dot [8].

For quantum dots with harmonic confinement by a potential $\frac{1}{2}m_{\rm e}\omega_0^2 r^2$, as a consequence of Kohn's theorem [9], the dipole operator D_ϱ excites only two collective states at energies $\omega_\pm = \sqrt{\omega_0^2 + \frac{1}{4}\omega_{\rm c}^2} \pm \frac{1}{2}\omega_{\rm c}$, where $\omega_{\rm c} = eB/m_{\rm e}c$ is the cyclotron frequency. If the confining potential is not harmonic, Kohn's theorem does not hold, and while on one hand, the energies of the modes depend on the number of electrons in the dot, on the other hand, a richer excitation spectrum appears.

Raman spectroscopy experiments on quantum dots have recently detected spin (magnetization) as well as charge modes and single particle (SP) excitations, and have followed their evolution with low magnetic fields [10–12]. The experiments have determined that the spin mode lies close to the uncorrelated single-electron excitations, which are much lower in energy than the magnetoplasmon mode, and that magnetoplasmons can also be detected by the use of spin-dependent probes. These are some basic results that any consistent theory of spin and charge excitations should describe.

The response to the spin-dependent dipole operator $D_m = \sum_i x_i \sigma_i^z$, where σ_i^z is the corresponding Pauli matrix, has been recently addressed by two of us [13] for the case of unpolarized quantum dots without magnetic field. Here we present an extension of that formalism to the case of a quantum dot subjected to a perpendicular magnetic field, which originates a B-dependent spin polarization in its ground state (GS). We use the time-dependent local spin-density approximation (TDLSDA) to obtain the response equations to a longitudinal field. By longitudinal we mean an external field which is either spin-independent or dependent on the spin component parallel to the magnetic field, i.e., the z component. To illustrate the relevant features of the TDLSDA response without excessive computational effort, we present results obtained for the particular case of 5 electrons in parabolic confinement, which is known to represent very well the experimental devices for small- and medium-sized dots.

2 TDLSDA

The description of adiabatic linear oscillations induced by external fields in the spin densities of an electronic system was studied some time ago [14, 15]. It required the generalization of density functional theory to explicitly include the electronic spin. When spin degeneracy is lost and the spin magnetization has a constant direction, the relevant vari-

ables for the description of the system are the spin densities $\varrho_\uparrow$ and $\varrho_\downarrow$ or, equivalently, the total density $\varrho = \varrho_\uparrow + \varrho_\downarrow$ and magnetization $m = \varrho_\uparrow - \varrho_\downarrow$.

2.1 Ground state

We consider a 2D quantum dot with a parabolic confining potential in the xy plane (with polar coordinates $r\,\theta$): $V^+(r) = \frac{1}{2} m_{\rm e}\,\omega_0^2\,r^2$. The spin densities ϱ_σ, with $\sigma = \uparrow, \downarrow$, are built from the set of self-consistent Kohn–Sham orbitals $\{\varphi_\alpha\}$. As a consequence of circular symmetry, the φ_α are eigenstates of the SP orbital angular momentum ℓ_z, i.e., $\varphi_\alpha(r,\theta) = u_{n\ell\sigma}(r) e^{-i\ell\theta}$, with $\ell = 0, \pm 1, \pm 2 \ldots$. Then, the GS electron density is given by $\varrho(r) = \sum_\alpha n_\alpha u_\alpha^2(r)$, while the GS spin magnetization is expressed in terms of the spin of orbital α, $\langle\sigma_z\rangle_\alpha$ as $m(r) = \sum_\alpha n_\alpha \langle\sigma_z\rangle_\alpha u_\alpha^2(r)$. The occupation factors n_α are those corresponding to the Fermi distribution at a given temperature T.

Within the symmetric gauge for the vector potential, the Kohn–Sham equations in the presence of a constant magnetic field B in the z direction are

$$\left[-\frac{1}{2}\nabla^2 + \frac{1}{2}\omega_{\rm c}\ell_z + \frac{1}{8}\omega_{\rm c}^2 r^2 + V^+(r) + V^H + \frac{\partial \mathcal{E}_{\rm xc}}{\partial \varrho} + \left(\frac{\partial \mathcal{E}_{\rm xc}}{\partial m} + \frac{1}{2} g^* \mu_{\rm B} B\right)\sigma_z\right]\varphi_\alpha = \epsilon_\alpha \varphi_\alpha \,, \quad (1)$$

where $V^H = \int {\rm d}\mathbf{r}\,' \varrho(\mathbf{r}\,')/|\mathbf{r} - \mathbf{r}\,'|$ is the Hartree potential. In (1), we have used modified effective units in terms of the parameters characterizing the host semiconductor medium. For GaAs, we have taken $\epsilon = 12.4$, $m^* = 0.067$, and $g^* = -0.44$, which yield an effective length unit (Bohr radius) $a_0^* = 97.9$ Å and an energy unit (Hartree) $H^* = 11.9\,{\rm meV} \approx 95.6\,{\rm cm}^{-1}$. The exchange-correlation energy density $\mathcal{E}_{\rm xc}(\varrho, m)$ has been constructed from the results of Tanatar and Ceperley [16] on the nonpolarized and fully polarized 2D electron gas in the same way as in [17], i.e., using the von Barth and Hedin [18] prescription to interpolate between both regimes.

2.2 Linear response

Following [14,15], we consider the variations $\delta\varrho_\sigma(\mathbf{r},\omega)$ induced in the GS spin densities $\varrho_\sigma(r)$ by an external spin-dependent field $Fe^{-i\omega t}$. We denote the nontemporal dependence as

$$F = \sum_\sigma f_\sigma(\mathbf{r})\,|\sigma\rangle\langle\sigma| \equiv \begin{pmatrix} f_\uparrow(\mathbf{r}) \\ f_\downarrow(\mathbf{r}) \end{pmatrix}. \quad (2)$$

For the dipole operators defined in the introduction, we then have $D_\varrho \equiv \begin{pmatrix} x \\ x \end{pmatrix}$ and $D_m \equiv \begin{pmatrix} x \\ -x \end{pmatrix}$. Notice that in (2) we have assumed that in longitudinal response theory, the external field is diagonal in spin space and thus can be represented as a two-component vector.

The spin-density correlation function $\chi_{\sigma\sigma'}$ relates the induced densities to the external field as

$$\delta\varrho_\sigma(\mathbf{r},\omega) = \sum_{\sigma'} \int {\rm d}\mathbf{r}\,' \chi_{\sigma\sigma'}(\mathbf{r},\mathbf{r}\,';\omega) f_{\sigma'}(\mathbf{r}\,') \,. \quad (3)$$

For free (non interacting) particles, a similar relation holds between the induced noninterating density $\delta\varrho_\sigma^{(0)}(\mathbf{r},\omega)$ and the noninteracting spin-density correlation function $\chi_{\sigma\sigma'}^{(0)}$, which is obtained from the Kohn–Sham SP orbitals

$$\chi_{\sigma\sigma'}^{(0)}(\mathbf{r},\mathbf{r}\,',\omega) = \delta_{\sigma,\sigma'} \sum_{\alpha\beta} (n_\alpha - n_\beta) \frac{\varphi_\alpha^*(\mathbf{r})\varphi_\beta(\mathbf{r})\varphi_\beta^*(\mathbf{r}\,')\varphi_\alpha(\mathbf{r}\,')}{\epsilon_\alpha - \epsilon_\beta + \omega + i\eta} \,, \quad (4)$$

where the label α (β) refers to an SP level with spin σ (σ'). Notice that $\chi_{\sigma\sigma'}^{(0)}$ is spin-diagonal in this case.

In TDLSDA, it is assumed that electrons respond as free particles to the modified mean field, not to the external one. This condition defines a new equation for the induced densities. Using a matrix notation in which space integrations are implicit, the TDLSDA equations are

$$\begin{pmatrix} \delta\varrho_\uparrow \\ \delta\varrho_\downarrow \end{pmatrix} = \begin{pmatrix} \delta\varrho_\uparrow^{(0)} \\ \delta\varrho_\downarrow^{(0)} \end{pmatrix} + \begin{pmatrix} \chi_{\uparrow\uparrow}^{(0)} & 0 \\ 0 & \chi_{\downarrow\downarrow}^{(0)} \end{pmatrix} \begin{pmatrix} K_{\uparrow\uparrow} K_{\uparrow\downarrow} \\ K_{\downarrow\uparrow} K_{\downarrow\downarrow} \end{pmatrix} \begin{pmatrix} \delta\varrho_\uparrow \\ \delta\varrho_\downarrow \end{pmatrix}. \quad (5)$$

The kernel $K_{\sigma\sigma'}$ is the residual two-body interaction

$$K_{\sigma\sigma'}(\mathbf{r}_1,\mathbf{r}_2) = \frac{1}{|\mathbf{r}_1 - \mathbf{r}_2|} + \left.\frac{\partial^2 \mathcal{E}_{\rm xc}(\varrho,m)}{\partial\varrho_\sigma \partial\varrho_{\sigma'}}\right|_{\rm gs} \delta(\mathbf{r}_1 - \mathbf{r}_2), \quad (6)$$

where

$$\frac{\partial^2 \mathcal{E}_{\rm xc}}{\partial\varrho_\sigma \partial\varrho_{\sigma'}} = \frac{\partial^2 \mathcal{E}_{\rm xc}}{\partial\varrho^2} + (\eta_\sigma + \eta_{\sigma'}) \frac{\partial^2 \mathcal{E}_{\rm xc}}{\partial\varrho\,\partial m} + \eta_\sigma \eta_{\sigma'} \frac{\partial^2 \mathcal{E}_{\rm xc}}{\partial m^2} \quad (7)$$

with $\eta_\uparrow = 1$, $\eta_\downarrow = -1$.

For a nonpolarized (fully spin-degenerate) system, one has $\chi_{\uparrow\uparrow}^{(0)} = \chi_{\downarrow\downarrow}^{(0)}$ and $\partial^2 \mathcal{E}_{\rm xc}/\partial\varrho\,\partial m|_{\rm gs} = 0$. It is easy to check that the matrix equation (5) reduces to two uncoupled equations for $\delta\varrho = \delta\varrho_\uparrow + \delta\varrho_\downarrow$ and $\delta m = \delta\varrho_\uparrow - \delta\varrho_\downarrow$, induced by D_ϱ and D_m, respectively. This constitutes the paramagnetic limit of the longitudinal response with uncoupled density and spin channels [13], in which the residual interaction consists of an exchange-correlation and a Coulomb direct term in one case, and of an exchange-correlation term only in the other.

In the general case, the two equations embodied in (5) are coupled and have to be treated simultaneously. An important simplification follows from noting that the fields D_ϱ and D_m couple only to the dipole components of the $\delta\varrho_\sigma$, $\chi_{\sigma\sigma'}$, and $K_{\sigma\sigma'}$ functions. In fact, the response to the $\ell = \pm 1$ fields,

$$D_\varrho^{(\pm 1)} = \frac{1}{2} r e^{\pm i\theta} \begin{pmatrix} 1 \\ 1 \end{pmatrix} \quad (8)$$

$$D_m^{(\pm 1)} = \frac{1}{2} r e^{\pm i\theta} \begin{pmatrix} 1 \\ -1 \end{pmatrix}, \quad (9)$$

can be obtained independently. For a polarized system having a nonzero magnetization in the GS, the $\ell = \pm 1$ modes are not degenerate, and give rise to two excitation branches with $\Delta L_z = \pm 1$, where L_z is the GS orbital angular momentum.

The dynamical polarizability $\alpha_{AB}(\omega)$ corresponding to the expectation value of field A with the densities induced by field B, where A and B are either D_ϱ or D_m, is given by

$$\alpha_{AB}(\omega) = -\left(f_\uparrow^{A*} f_\downarrow^{A*}\right) \begin{pmatrix} \delta\varrho_\uparrow^B \\ \delta\varrho_\downarrow^B \end{pmatrix} \tag{10}$$

Their imaginary parts are related to the strength functions as $S_{AB}(\omega) = \frac{1}{\pi}\mathrm{Im}[\alpha_{AB}(\omega)]$.

3 Numerical results

We report in the following numerical results for a quantum dot of 5 electrons confined in a parabolic potential with $\omega_0 = 4.28\,\mathrm{meV}$. A systematic analysis for different confining potentials and a higher number of electrons will be reported elsewhere. Figure 1 shows the dipole strength functions for different magnetic fields. The numerical results have been obtained using a small but finite temperature $T \leq 0.1\,\mathrm{K}$ and a parameter $\eta = 0.006\ \mathrm{H}^*$ in (4). Solid and dotted lines correspond to $S_{\varrho\varrho}$ and S_{mm}, respectively, while the free particle response is represented by the dashed line. We first notice that for $B = 0$, the density response $S_{\varrho\varrho}$ has a single peak at exactly ω_0, and for $B \neq 0$, two peaks (magnetoplasmons) occur at energies $\omega_\pm = \sqrt{\omega_0^2 + \frac{1}{4}\omega_\mathrm{c}^2} \pm \frac{1}{2}\omega_\mathrm{c}$. These are well-known facts which, together with the fulfillment of the the f-sum rule in both channels, constitute a test of our calculation.

The free response is concentrated in a small interval around 2.5 meV at $B = 0$, and for increasing B, it splits into two regions; the higher the magnetic field, the larger the separation between them. This is naturally associated with the appearance of quasi-SP Landau bands and two possible types of electron-hole transition: the low-energy intraband transition, and the high-energy interband transition, whose energy tends to $\hbar\omega_\mathrm{c}$ as B increases.

A more interesting behavior is exhibited by the spin response S_{mm}, whose peaks are located at energies somewhat smaller than those of the free response. The different shifts of the density and spin responses from the free one are due to the well-known differences in the effective residual interaction in both channels, i.e., the interaction is weak and attractive in the spin channel, because only the exchange-correlation energy contributes to it, and strong and repulsive in the density channel, because direct terms also contribute.

The magnetoplasmon peaks can also be seen in the spin response, although generally as low-intensity peaks. This indicates that the magnetoplasmon mode can be excited by a spin-dependent probe and is a manifestation of the coupling between channels, which has been seen experimentally [12]. For a parabolic confinement, the symmetric

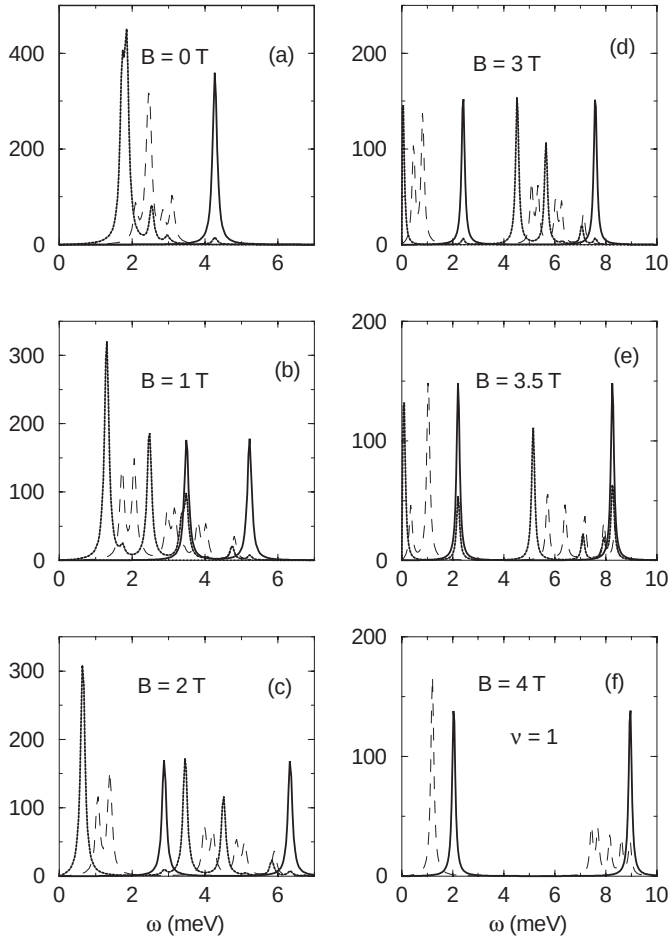

Fig. 1. Dipole strength in effective atomic units of the 5-electron dot, discussed in the text, as a function of energy (meV). Solid lines correspond to $S_{\varrho\varrho}$, i.e., to the density response to D_ϱ, and dotted lines to S_{mm}, i.e., to the spin response to D_m. Dashed lines represent the free particle strength function.

situation, namely the manifestation of the spin peaks in the density response, is forbidden by Kohn's theorem.

The manifestation of magnetoplasmons in the spin response is sizeably enhanced because of a resonance mechanism that occurs when the magnetoplasmon and particular spin excitations are close in energy. This type of enhancement can be seen in the spin response at $B = 1\,\mathrm{T}$ (panel b of Fig. 1). The strength of these peaks also increases as the dot becomes more and more spin-polarized with higher magnetic fields (panel e).

The B dispersion of the main peaks in both spin and density channels is shown in Fig. 2. The lines are drawn as a guide to the eye. Quite interestingly, the energy of the lower spin mode essentially vanishes for magnetic fields in the region 3–3.5 T. This indicates that at these magnetic fields, the GS we have used (with circular symmetry) is no longer stable against spin-density dipole oscillations. We remark that at $B = 0$, a spin-wave instability of similar type has been recently found in [17] to appear for increasing values of the r_s parameter (decreasing electronic surface densities). Our results indicate that this instabil-

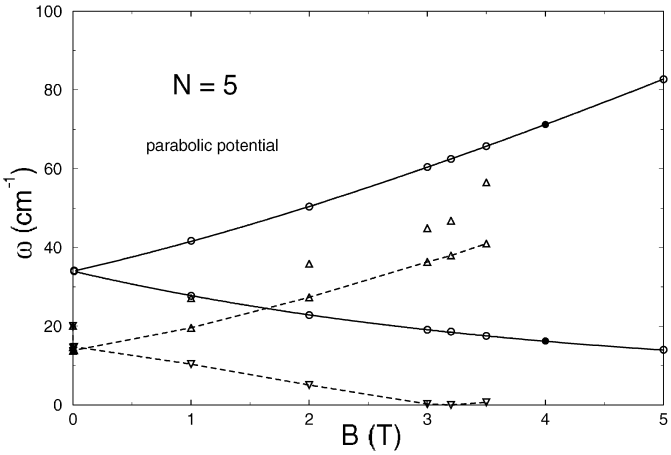

Fig. 2. B dispersion of the main peaks of the dot of Fig. 1. The circles correspond to density modes and the triangles to spin modes. The solid symbol corresponds to the filling factor $\nu = 1$, and the lines connect the more intense peaks.

ity can also be induced by applying a magnetic field to the quantum dot.

At $B = 4$ T, the dot becomes fully spin-polarized, with occupation of the five lowest angular momentum levels of the first Landau band. It thus corresponds to filling factor $\nu = 1$. In this case, the spin and density responses coincide, and the surviving excitations correspond to Kohn's magnetoplasmon modes.

4 Summary

In this contribution, we have discussed the longitudinal spin and density responses of a quantum dot in a magnetic field within TDLSDA. To our knowledge, this is the first application of TDLSDA to the description of spin modes in quantum dots at $B \neq 0$. As an application, we have obtained the dipole modes for a dot made of 5 electrons in a parabolic confining potential.

For a partially polarized dot, spin and density channels are generally coupled. In parabolic confinement, this implies that magnetoplasmons can also be seen in the spin channel. In this case, the microscopic TDLSDA reproduces the exact magnetoplasmon energies given by Kohn's theorem.

The B dispersion of the spin modes shows that the circularly symmetric dot becomes unstable against dipole spin-density waves for B larger than a certain value. At full polarization the theory gives the magnetoplasmons as the only dipole excitations. Work to extend the present study to other confining potentials and to the spin transverse response in larger dots is underway.

This work has been performed under grants PB95-1249 and PB95-0492 from CICYT, and 1998SGR00011 from Generalitat de Catalunya. A.E. acknowldeges support from DGES, Spain.

References

1. W.A. de Heer: Rev. Mod. Phys. **65**, 611 (1993); M. Brack: Rev. Mod. Phys. **65**, 677 (1993)
2. Ch. Sikorski, U. Merkt: Phys. Rev. Lett. **62**, 2164 (1989)
3. T. Demel, D. Heitmann, P. Grambow, K. Ploog: Phys. Rev. Lett. **64**, 788 (1990)
4. D. Broido, K. Kempa, B. Bakshi: Phys. Rev. B **42**, 11 400 (1990)
5. P.A. Maksym, T. Chakraborty: Phys. Rev. Lett. **65**, 108 (1990)
6. V. Gudmundsson, R.R. Gerhardts: Phys. Rev. B **43**, 12 098 (1991)
7. V. Shikin, S. Nazin, D. Heitmann, T. Demel: Phys. Rev. B **43**, 11 903 (1991)
8. U. Merkt: Physica B **189**, 165 (1993)
9. W. Kohn: Phys. Rev. B **123**, 1242 (1961)
10. R. Strenz, U. Bockelmann, F. Hirler, G. Abstreiter, G. Böhm, G. Weimann: Phys. Rev. Lett. **73**, 3022 (1994)
11. D.J. Lockwood, P. Hawrylak, P.D. Wang, C.M. Sotomayor-Torres, A. Pinczuk, B.S. Dennis: Phys. Rev. Lett. **77**, 354 (1996)
12. C. Schüller, K. Keller, G. Biese, E. Ulrichs, L. Rolf, C. Steinebach, D. Heitmann: Phys. Rev. Lett. **80**, 2673 (1998)
13. Ll. Serra, E. Lipparini: Europhys. Lett. **40**, 667 (1997)
14. A.R. Williams, U. von Barth: in *Theory of the inhomogeneous electron gas*, ed. by S. Lundqvist, N.H. March (Plenum, New York 1983) p. 231
15. A.K. Rajagopal: Phys. Rev. B **17**, 2980 (1978)
16. B. Tanatar, D.M. Ceperley: Phys. Rev. B **39**, 5005 (1989)
17. M. Koskinen, M. Manninen, S.M. Reimann: Phys. Rev. Lett. **79**, 1389 (1997)
18. U. von Barth, L. Hedin: J. Phys. C **5**, 1629 (1972)